Power Law Guided Dynamic Sifting for Efficient Attention

Nirav Koley[*], **Prajwal Singhania**[*], **Abhinav Bhatele**

Department of Computer Science, University of Maryland
College Park, MD 20742
`prajwal@umd.edu`, `bhatele@cs.umd.edu`

Abstract

Efficient inference on GPUs using large language models remains challenging due to memory bandwidth limitations, particularly during data transfers between High Bandwidth Memory (HBM) and SRAM in attention computations. Approximate attention methods address this issue by reducing computational and memory overhead but often rely on expensive top-k operations, which perform poorly on GPUs. We propose SiftAttention, a novel approximate attention method that replaces the top-k step with a computationally efficient element-wise filtering operation based on a threshold value. Our intuition for doing this is based on our empirical observation that the τ-th quantile of attention scores follows a predictable power-law over sequential generation steps. Exploiting this insight, our approach dynamically estimates a threshold value per prompt at each generation step. Only attention scores above this threshold and their corresponding value vectors are loaded/used to compute the attention output, reducing data movement between HBM and SRAM. Our evaluation demonstrates that SiftAttention preserves model quality better than existing approximate attention methods while reducing memory bandwidth usage when loading value vectors.

1 Introduction

Large language models (LLMs) have transformed natural language processing and many other areas in computer science, achieving state-of-the-art results across a wide range of tasks. Powered by the transformer architecture [24], these models leverage the self-attention mechanism [2] to learn complex language patterns. As the sizes of large language models (LLMs) have grown from millions to hundreds of billions of parameters, their computational, memory, and consequently energy demands have also increased significantly.

The self-attention mechanism, originally applied to relatively small models, now poses a major efficiency bottleneck, especially during auto-regressive generation for long sequence lengths. At each generation step, the attention mechanism computes a weighted sum over all previous token states stored in a key-value (KV) cache. Transferring this data from GPU High Bandwidth Memory (HBM) to on-chip SRAM is costly and leads to significant memory bandwidth bottlenecks [8]. Additionally, it requires dot-product computation between the current input and all previous token states, leading to quadratic computational complexity with respect to sequence length.

Several methods have been proposed to address the computational challenges associated with the attention mechanism. Our work focuses on a particular class of methods that aim to approximate the attention computation by reducing the number of tokens used in the attention computation, trading

[*]Equal contribution

Preprint. Under review.

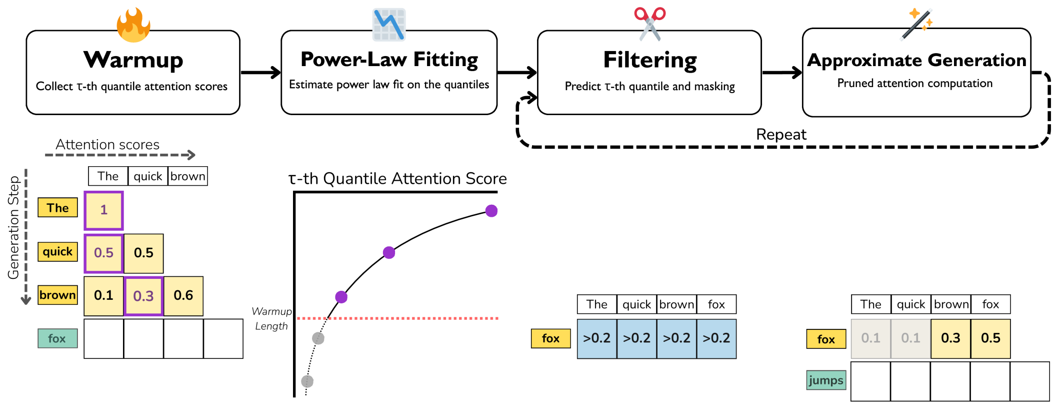
Warmup
Collect τ-th quantile attention scores
Power-Law Fitting
Estimate power law fit on the quantiles
Filtering
Predict τ-th quantile and masking
Approximate Generation
Pruned attention computation
Repeat
Attention scores
Generation Step
The
quick
brown
fox
jumps
τ-th Quantile Attention Score
Warmup Length
>0.2

Figure 1: Overview of SiftAttention

off accuracy for efficiency. These methods either prune the KV-cache permanently [29] for memory savings or dynamically select a subset of tokens per generation step [18, 10, 22] to reduce the amount of key-value pairs to attend to. The latter set of methods typically use a top-k selection operation to select the top k tokens with the highest attention scores, which is inefficient on GPUs due to thread-synchronization overheads. We introduce *SiftAttention*, a new approximation strategy that replaces top-k with an element-wise filtering operation.

Our approach is based on a key empirical finding: the τ-th quantile of attention scores follow a predictable power-law decay over generation steps. This trend is consistent across models and datasets and enables us to estimate quantile thresholds dynamically using a small warmup window. Based on this insight, we design SiftAttention with two-phases: a short *warmup*, and an *approximate generation* phase. During the warmup, seen on the left of Figure 1, we record the τ-th quantile of attention scores at each generation step and fit a power-law curve to these samples. During approximate generation, seen on the right of Figure 1, we use our fitted power-law to predict the τ-th quantile of attention scores at each generation step, retaining only those keys whose attention weights are above this threshold and loading their corresponding value vectors to SRAM.

We evaluate SiftAttention on perplexity, short-context, and long-context generation tasks across multiple models. Our results demonstrate that SiftAttention maintains a high level of model quality, with negligible degradation in perplexity (within 0.1) and task-specific metrics. We also implement a fused Triton [1] kernel for SiftAttention to demonstrate that our method reduces data movement in the GPU memory hierarchy when loading value vectors, similar to other top-k methods.

In summary, our contributions are as follows:

- We discover and analyze that attention score quantiles follow a power-law trend across generation steps and demonstrate that this can be estimated using a few warmup steps.
- We propose SiftAttention, an approximate attention method that avoids the expensive top-k sorting operation by compute-efficient filtering using a quantile-based threshold value.
- We demonstrate SiftAttention's effectiveness across multiple benchmarks, including perplexity, short-context, and long-context generation tasks, and showing that it maintains model quality better than existing approximate attention methods.

2 Background and Related Work

Auto-regressive Decoding: During auto-regressive decoding, transformers generate one token at a time by applying causal self-attention over all previously generated tokens [24]. At generation step S, the attention output is computed as:

$$\mathbf{o}_S = \mathrm{softmax}\left(\frac{\mathbf{q}_S \mathbf{K}_{:S}^T}{\sqrt{D}}\right)\mathbf{V}_{:S} \tag{1}$$

where $\mathbf{q}_S \in \mathbb{R}^{1\times D}$ is the query, and $\mathbf{K}_{:S}, \mathbf{V}_{:S} \in \mathbb{R}^{S\times D}$ are the key and value caches, respectively.

Power-Law Decay: A power-law decay describes relationships of the form: $y = \alpha \cdot x^{-\beta}$, where $\alpha, \beta \in \mathbb{R}$ and $\alpha, \beta > 0$. Assuming a multiplicative error in y, this can be linearized in log-log space to enable efficient parameter estimation via linear regression, as:

$$\log y = \log \alpha - \beta \log x \tag{2}$$

2.1 Related Work

Empirical analyses of pre-trained transformers show that only a small subset of past keys receive the majority of the attention weight [14]. This has motivated a range of approximate attention methods that exploit this sparsity to either reduce the cost of full attention [7, 18, 22, 10] or prune unimportant key-value pairs to reduce memory overhead [12, 29]. While traditional methods focus on patterns within a single generation step, very few methods explore how attention scores evolve across generation steps. To the best of our knowledge, our work is the first to empirically demonstrate that attention score quantiles exhibit a predictable power-law decay over time and to then use this insight to sparsify attention scores dynamically during inference.

The original Top-k method [7] selects the most relevant k keys via a global sort over exact attention scores. Despite impressive downstream performance, the top-k operation introduces a full-row dependency that limits parallel execution on modern GPUs. While recent methods like Loki [22] and SparQ [18] aim to approximate attention scores in low-dimensional subspaces, they still rely on the top-k operation to select the most important scores, which remains a bottleneck [28]. SiftAttention aims to replaces the top-k operation with a simple element-wise threshold comparison, making it highly parallelizable on GPUs.

Token-eviction methods, such as Scissorhands [12] and the H_2O [29], reduce memory usage by deleting tokens permanently, which can lead to a significant degradation in model quality. In contrast, SiftAttention retains the full KV-cache and sparsifies only during attention computation, prioritizing task performance over memory savings.

The most closely related works to SiftAttention are LeOPArd [11] and Top-θ Attention [3]. LeOPArd learns fixed thresholds per transformer layer during training and drops scores below them at inference time, achieving $1.9\times$ speedups on specialized hardware. However, it introduces training/fine-tuning overhead and lacks flexibility to adapt thresholds based on sequence specific dynamics. Top-θ estimates thresholds per head, layer, and generation step using an offline calibration set with some limited online fine-tuning. This requires storing calibrated thresholds for all generation steps, which can be memory-intensive for long contexts. SiftAttention is the first fully online, dataset-agnostic, and model-agnostic sparsification technique that doesn't require any offline step which can dynamically adapt to sequence/query dynamics.

3 Power-Law Analysis

In this section, we investigate the evolution of attention score quantiles over sequential generation steps and discover a consistent empirical pattern: the τ-th quantiles exhibit a decay that closely follows a power-law. We then show the efficacy of capturing this trend using a power-law fit and introduce a method to estimate the parameters of this fit with comparatively minimal overhead.

3.1 Analyzing the Temporal Decay of Attention Score Quantiles

To examine whether attention scores exhibit consistent and predictable behavior over generation steps, we analyze them across multiple models on a perplexity evaluation task. Specifically, we focus on specific quantiles of the attention scores and fit power-law models to capture their decay over time.

Experimental Setup: We evaluate five models spanning a diverse range of architectures and scales: Llama-3.1 (8B Instruct and 70B Instruct), Llama-3.2 3B Instruct, Mistral 7B, Qwen2.5 7B [6, 9, 26]. Evaluations are conducted on WikiText-2 (test split) [13] and C4 (custom split) [17], using a perplexity evaluation pipeline. Each model is run on sequences of length 4096 tokens. The experiments are run on Nvidia GH200 and H100 GPUS, with larger models distributed across multiple GPUs using AxoNN [19, 21].

We track the attention scores at selected quantile levels τ: 0.5, 0.75, and 0.875, denoting the τ-th quantile at generation step i as $\theta_{i,\tau}$. For each prompt, layer, and head, we extract the quantile time series and fit a power-law curve of the form $\hat{\theta}_{i,\tau} \approx \alpha \cdot i^{-\beta}$. We fit the power-law by performing linear regression in log-log space, which enables both efficient closed-form estimation using standard tensor operations and implicitly models multiplicative noise. To evaluate the quality of the fit, we compute the coefficient of determination (R^2), defined as:

$$R^2 = 1 - \frac{\sum_i (\ell_i - \hat{\ell}_i)^2}{\sum_i (\ell_i - \bar{\ell})^2} \tag{3}$$

where ℓ_i is the logarithm of the τ-th quantile score at generation step i, $\ell_i = \log(\theta_{i,\tau})$, $\hat{\ell}_i$ is the logarithm of the predicted value from the power-law fit, and $\bar{\ell}$ denotes the mean value of ℓ_i. This metric is computed for each prompt, layer, and head.

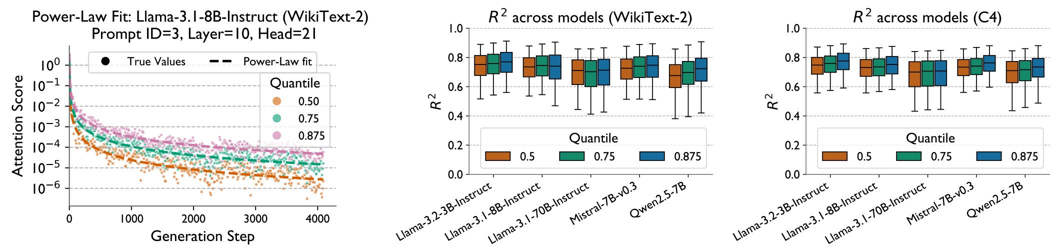

Figure 2: Power-Law fit for attention score quantiles (log y-scale) over generation steps for Llama-3.1 8B on WikiText-2 (left). Distribution of R^2 values for power-law fits across prompts, layers, and heads for various models on WikiText-2 (middle) and C4 (right) datasets. Boxes denote the median, 25^{th} and 75^{th} percentiles, and the whiskers denote the 5^{th} and 95^{th} percentile values.

Analysis: We begin by analyzing the temporal trend in attention score quantiles for Llama-3.1 8B on WikiText-2 (Figure 2, left). The plot depicts the evolution of the 0.5, 0.75, and 0.875 quantiles over generation steps for a specific prompt, layer, and head index. Each line reflects a power-law fit, plotted alongside the true quantile values. For visual clarity, the generation steps are down-sampled to onlyshow every 10^{th} step. Despite some local noise, we observe a remarkably consistent decline in quantile values over time, with high correspondence to the fitted power-law curves. Similar trends for other models can be found in appendix A.

To demonstrate the generalizability of this observed trend, we report the R^2 values for power-law fits aggregated across all layers, heads, and prompts for different models (Figure 2, middle and right). Across models of different architectures and sizes, the power-law fit consistently achieves high R^2 values, with median values between 0.6 and 0.8. Although a small fraction of fits exhibit lower quality—particularly at the 5th percentile, which can fall to around 0.4 - the overall distribution of R^2 indicates that the power-law fit is a good approximation for the decay of attention score quantiles over generation steps. This trend further holds across both datasets used. This consistent result across diverse settings supports the hypothesis that the quantile decay might be a fundamental and architecture-agnostic property of transformer models.

This insight has significant practical implications: it suggests that the trajectory of attention score quantiles can be predicted reliably across different models, potentially enabling efficient threshold estimation without the need for an expensive top-k operation at each step. Next, we explore the possibility of estimating the power-law parameters using a small warmup phase.

3.2 Estimating Power-Law Fit Parameters with a Warmup Phase

Having established that attention score quantiles follow an approximate power-law decay, we now focus on estimating the parameters of this curve during inference. We explore whether a small number of initial generation steps can be used to estimate the power-law parameters accurately.

Following the experimental setup described in Section 3.1, we now fit the power-law function using only the values from the first w generation steps - henceforth referred to as the warmup phase. We evaluate four warmup lengths: w: 64, 128, 256, and 512. The power-law parameters are estimated using only the warmup steps, but the resulting fit is evaluated across all generation steps (including both warmup and post-warmup) by computing the coefficient of determination (R^2). This warmup-based R^2 captures out-of-sample generalization and as a result, R^2 values can be negative when the

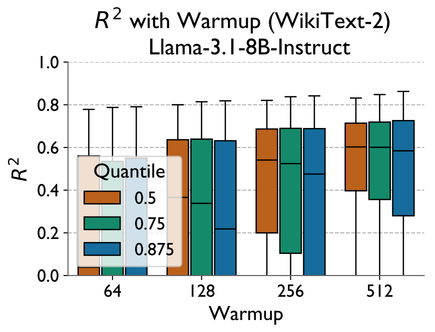

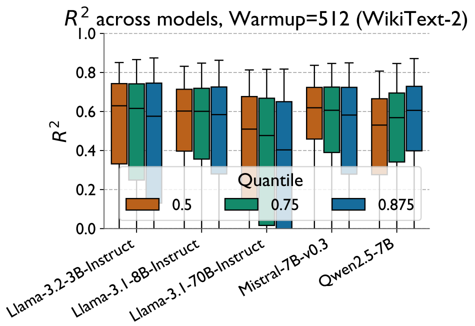

Figure 3: R^2 of power-law fits for attention score quantiles with warmup. Left: R^2 distribution for Llama-3.1-8B-Instruct on WikiText-2, evaluated across warmup sizes of 64, 128, 256, and 512 steps. Right: Fit quality across models with a warmup of 512. Longer warmups consistently yield stronger fits across models.

power-law fit performs worse than simply predicting the mean of the log-quantile values across the full sequence.

Figure 3 (left) shows how fit quality varies with the number of warmup steps for Llama-3.1-8B-Instruct on WikiText-2. With short warmup lengths (e.g., w =64), the R^2 values are often low, with a significant fraction falling below zero (truncated in the plot to the range $[0, 1]$). As the warmup length increases, the fit quality improves steadily. The same pattern can be seen across various models, the results of which are shown in appendix A. With w =512, the median R^2 across all quantiles approaches or exceeds 0.6, indicating strong generalization. Notably, 512 warmup steps still correspond to just 12.5% of the full 4096-token sequence, suggesting that accurate power-law parameter estimation requires only a small fraction of the total generation steps. Later, we will see that empirically, this is an adequate warmup length to achieve high downstream performance.

4 SiftAttention: Power-Law Guided Dynamic Filtering

In this section, we introduce SiftAttention, an approximate attention mechanism that exploits the power-law behavior of attention score distributions. We describe its two-phase design: a warmup phase for estimating power-law parameters, followed by an approximate generation phase that uses these estimates to prune attention computations efficiently. We also analyze the computational complexity of SiftAttention and discuss its implementation in practical settings.

4.1 Two-Phase Algorithm Design

SiftAttention operates in two distinct phases: a *warmup* phase (Algorithm 1) and an *approximate* generation phase (Algorithm 2).

Warmup Phase: During the warmup phase, we first compute the exact attention scores using the dot product of query and key vectors in the KV-Cache (Lines 1–2), followed by a softmax operation (Line 3). We then record the τ-th quantile of the computed attention scores for each prompt, layer, and head (Lines 4–5). This step is repeated until the warmup phase ends ($S \leq w$).

At the end of the warmup phase, we fit a power-law curve to these recorded quantile values across generation steps to obtain parameters α and β (Line 7). The fitting is performed efficiently by applying a logarithmic transform to both the generation step index S and quantile values, followed by linear regression in the subsequent log-log space. This method provides a closed-form solution using standard tensor operations, eliminating iterative optimization, and aligns naturally with the multiplicative noise assumption inherent in modeling probabilities.

Approximate Generation Phase. Once the warmup phase ends and the power-law parameters have been fit, the model enters the approximate generation phase (Algorithm 2). At each subsequent generation step, we use the learned power-law model to estimate the τ-th quantile of attention scores

Algorithm 1 SiftAttention: Warmup Phase

```
Input: At the $S^{th}$ step - Input: $\mathbf{x}_S \in \mathbb{R}^{1\times D}$, KV-cache: $\mathbf{K}_{:S-1}, \mathbf{V}_{:S-1} \in \mathbb{R}^{(S-1)\times D}$, Warmup
    Steps $w$, Quantile Level $\tau$, Past Quantile Scores: $\boldsymbol{\theta}_{:S-1} \in \mathbb{R}^{(S-1)\times 1}$
Ensure: $S \leq w$
 1: $\mathbf{q}_S, \mathbf{k}_S, \mathbf{v}_S \leftarrow \textsc{ComputeQKV}(\mathbf{x}_S)$
 2: $\mathbf{K}_{:S} \leftarrow \textsc{append}(\mathbf{K}_{:S-1}, \mathbf{k}_S), \mathbf{V}_{:S} \leftarrow \textsc{append}(\mathbf{V}_{:S-1}, \mathbf{v}_S)$
 3: $\boldsymbol{a}_S \leftarrow \textsc{softmax}\left(\frac{\mathbf{q}_S \mathbf{K}_{:S}^\top}{\sqrt{D}}\right)$
 4: $\theta_S \leftarrow \textsc{Quantile}(\boldsymbol{a}_S, \tau)$                    ▷ $\tau$-th quantile of attention scores
 5: $\boldsymbol{\theta}_{:S} \leftarrow \textsc{Concat}(\boldsymbol{\theta}_{:S-1}, \theta_S)$
 6: if $S = w$ then                                                  ▷ Warmup complete
 7:     $\alpha, \beta \leftarrow \textsc{FitPowerLaw}(\boldsymbol{\theta}_{:S})$
 8:     return $\boldsymbol{a}_S \mathbf{V}_{:S}, \alpha, \beta$
 9: else
10:     return $\boldsymbol{a}_S \mathbf{V}_{:S}$
11: end if
```

Algorithm 2 SiftAttention: Approximate Generation Phase

```
Input: At the $S^{th}$ step - Input: $\mathbf{x}_S \in \mathbb{R}^{1\times D}$, KV-cache: $\mathbf{K}_{:S-1}, \mathbf{V}_{:S-1} \in \mathbb{R}^{(S-1)\times D}$, Warmup
    Steps $w$, Powerlaw Fit Parameters - $\alpha, \beta$
Ensure: $S > w$
 1: $\mathbf{q}_S, \mathbf{k}_S, \mathbf{v}_S \leftarrow \textsc{ComputeQKV}(\mathbf{x}_S)$
 2: $\mathbf{K}_{:S} \leftarrow \textsc{Append}(\mathbf{K}_{:S-1}, \mathbf{k}_S), \quad \mathbf{V}_{:S} \leftarrow \textsc{Append}(\mathbf{V}_{:S-1}, \mathbf{v}_S)$
 3: $\boldsymbol{a}_S \leftarrow \textsc{softmax}\left(\frac{\mathbf{q}_S \mathbf{K}_{:S}^\top}{\sqrt{D}}\right)$
 4: $\eta_S \leftarrow \alpha \cdot S^{-\beta}$                                  ▷ Power-Law Estimation of Quantile
 5: $\textbf{indices} \leftarrow \{i \mid \boldsymbol{a}_S[i] > \eta_S\}$                              ▷ Filtering
 6: $\boldsymbol{a}'_S \leftarrow \boldsymbol{a}_S[\textbf{indices}], \quad \mathbf{V}'_{:S} \leftarrow \mathbf{V}_{:S}[\textbf{indices}]$        ▷ Retain only the indices above threshold
 7: return $\boldsymbol{a}'_S \mathbf{V}'_{:S}$
```

based on the current step index (Line 4). This predicted quantile serves as a dynamic threshold that adapts over time, reflecting the prior empirical observations in attention score distributions.

Using this threshold, we prune the attention weights by zeroing out all values below the predicted quantile (Line 5). Only the attention scores above the threshold are retained, and the corresponding value vectors are extracted from the KV-cache (Line 6). This selective sparsification reduces the number of values that need to be loaded from high-bandwidth memory (HBM) into on-chip SRAM, just as in top-k methods. Finally, the attention output is computed using only the surviving attention scores and their associated value vectors (Lines 7).

4.2 Computational Cost Analysis

We now present a run-time cost analysis of SiftAttention, compared to the Top-k method. Let S be the total number of generation steps (or tokens in the KV-cache), w the number of warmup steps.

The warmup phase of SiftAttention and the Top-k method are almost identical, with two main differences: SiftAttention requires an extra step of storing the τ-th quantile of attention scores at each step, and the final value projection uses all the attention scores (Line 8 & 10, Algorithm 1) (as opposed to Top-k which uses a fixed k scores). Given that the quantile score can be directly stored in a buffer, without any additional copying, we can approximate the difference in runtimes as:

$$T_{\text{SiftAttention, Warmup}} - T_{\text{Top-}k\text{ Attention}} \approx (T_{\text{proj-}V} - T_{\text{proj-}V'}) \tag{4}$$

where $T_{\text{proj-}V}$ is the runtime cost of computing the vector-matrix product between the full attention scores and the value matrix, and $T_{\text{proj-}V'}$ is the cost of the same operation between the pruned attention scores and the value matrix.

During the approximate generation phase, SiftAttention thresholds the attention scores before value projection, instead of a top-k selection, and thus the difference in runtime can be approximated as:

$$T_{\text{SiftAttention, ApproxGen}} - T_{\text{Top-}k\text{ Attention}} \approx T_{\text{threshold}} - T_{\text{top-}k} \tag{5}$$

All the other operations are the same as in the Top-k method. Based on these approximations, we can compare the runtime of SiftAttention with the Top-k method over S generation steps (with w warmup steps), as follows:

$$T^{(S)}_{\text{SiftAttention}} - T^{(S)}_{\text{TopKAttention}} \approx w(T_{\text{proj-}V} - T_{\text{proj-}V'}) + (S - w)(T_{\text{threshold}} - T_{\text{top-}k}) + T_{\text{power-law-fit}} \tag{6}$$

Given $w \ll S$, the first term becomes negligible and the power-law fit is a one-time operation using fast tensor operations. Thus, the runtime difference is dominated by the last two terms:

$$T^{(S)}_{\text{SiftAttention}} - T^{(S)}_{\text{TopKAttention}} \approx (S - w)T_{\text{threshold}} - T_{\text{top-}k} \tag{7}$$

Since thresholding can be done element-wise, in parallel and does not require sorting like top-k, we have $T_{\text{top-}k} > T_{\text{threshold}}$, leading a negative RHS in the above equation.

4.3 Implementation Details

Next, we discuss key implementation details of SiftAttention. We develop a Triton-based kernel for the approximate generation phase. For the warmup phase and power-law fit, we use standard PyTorch [16] operations with `torch.compile` [23] enabled for performance. A key thing to note is that our triton kernel is not the most efficient implementation of this approach. The reason being that, for an efficient implementation of SiftAttention (and any top-k based approach), the pruned attention scores and value vectors need to be compacted in memory (Line 6, Algorithm 2). If this is not done, the resulting vector-matrix product will be a sparse-sparse product, which is not efficient on modern GPU architectures when compared to a dense vector-matrix products. Triton does not allow for fine-grained manipulation of shared memory, leading us to write the intermediate indices in global memory. This limitation is not present if implemented directly in CUDA, and we leave this as future work. Due to this, we will see later that our approach cannot compete with highly optimized fused standard attention kernels. However, our implementation works as a proof-of-concept, showing that our approach can lead to a reduction in HBM to SRAM data movement, as seen in our experiments.

5 Experimental Setup

For model quality benchmarking, we evaluate SiftAttention on two categories of tasks: perplexity and downstream generation. Evaluations are conducted on a subset of open-weight models: Llama-3.1 (8B Instruct and 70B Instruct), Llama-3.2 3B Instruct, Mistral 7B, Qwen2.5 7B [6, 9, 26]. Due to tokenizer incompatibility, the Qwen model is excluded from downstream generation tasks. The main text presents results for the Llama family, while results for other models are provided in appendix B.

We evaluate perplexity using the WikiText-2 [13] dataset. Downstream generation evaluations are divided into short-context and long-context settings. Short-context tasks include IFEval [30] and MATH-Hard [4], selected from the Hugging Face Open LLM Leaderboard [5]. The long-context setting employs LongGenBench [25], capped at 4096 tokens due to computational constraints.

We compare against three baselines: Full Attention (no approximations), Top-k Attention [7], and H_2O [29]. H_2O is excluded for Llama-3.1-70B-Instruct due to its lack of multi-GPU support, and from downstream generation tasks due to computational constraints. Top-k is evaluated only on perplexity and short-context tasks, due to computational constraints. To ensure fair evaluation, we discard samples where the number of generated tokens is less than the maximum warmup length in our experiments and report metrics only on valid completions, for both SiftAttention and all baselines. For Top-k we use $k \in \{0.5, 0.25, 0.125, 0.05\}$, and an analogous retain budget for H_2O. For SiftAttention, we use $\tau \in \{0.5, 0.75, 0.875, 0.95\}$ and warmup $w \in \{16, 32, 64, 128, 256, 512\}$.

For runtime benchmarking, we evaluate our Triton-based implementation of the approximate generation phase of SiftAttention on a micro-benchmark, written using Triton's benchmarking utilities. We compare our method against the fused scaled dot-product attention kernel (SDPA) from PyTorch. We enable `torch.compile` with `max-autotune` for both implementations. We profile the memory transfer volume using Nsight Compute [15]. Model quality runs are performed on GH200, and H100 GPUs. Runtime experiments are performed on A100 GPUs. Bigger models are parallelized across 4 H100 GPUs, using AxoNN [20, 19].

6 Results

We now compare SiftAttention against full attention and other baselines, and evaluate the performance of our Triton-based implementation relative to PyTorch's fused scaled dot-product attention kernels.

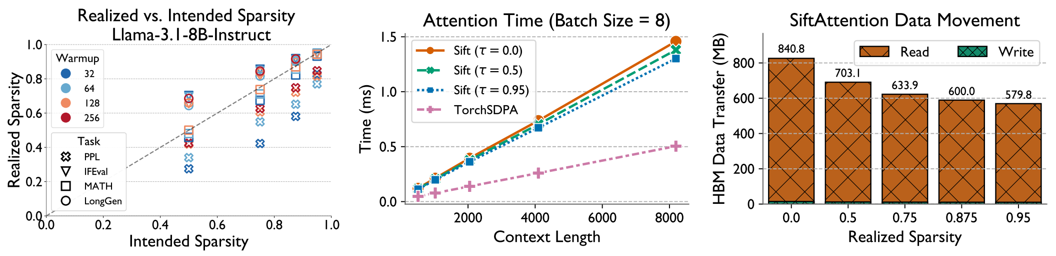

Figure 4: (Left) SiftAttention Intended vs. Realized sparsity across tasks and warmup lengths for Llama-3.1–8B-Instruct. (Middle) Post-warmup attention latency of our Triton-based SiftAttention implementation, compared to PyTorch's fused SDPA across varying context lengths (Batch Size = 8). (Right) HBM data transfer volume as a function of realized sparsity (Context Length = 8192), showing reduced memory reads with increased sparsity.

Intended vs. Realized Sparsity: We begin by distinguishing between intended sparsity, set by hyper-parameters (e.g., k in Top-k, τ in SiftAttention), and realized sparsity, the actual fraction of filtered tokens during inference. For static methods like Top-k and H_2O, intended and realized sparsity are equal by construction. However, in SiftAttention, sparsity is determined dynamically based on thresholding learned from power-law fits and may deviate from the intended sparsity.

We compute realized sparsity as the average ratio of pruned keys to total keys across all generation steps and samples. Figure 4 (left) shows this relationship for SiftAttention on Llama-3.1-8B-Instruct across various tasks and warmup lengths. Perplexity-oriented tasks tend to undershoot the intended sparsity, while downstream tasks like IFEval and LongGenBench often surpass it. While we do not yet have a theoretical explanation for these task-specific trends, a consistent observation is that longer warmup phases yield realized sparsity closer to the target. This aligns with earlier findings that longer warmups lead to better power-law fits for attention quantiles. Going forward, we report realized sparsity when comparing SiftAttention with baselines to keep comparisons fair.

Runtime and Data Transfer Volume Evaluation: Figure 4 (middle) compares SiftAttention's runtime (post-warmup) against PyTorch's fused Scaled Dot-Product Attention (SDPA) kernel (exact attention). As discussed in Section 4.3, due to Triton's limited support for shared memory and compaction, our kernel is slower. However, SiftAttention's runtime improves with sparsity: from 1.46 ms to 1.30 ms (10% reduction) at context length 8192. Investigating further, Figure 4 (right) shows that this gain stems from reduced HBM data transfer—falling from 840.8 MB to 579.8 MB (31% reduction) with increasing sparsity. This demonstrates that SiftAttention is able to reduce the HBM to SRAM data movement, as well as other top-k based approaches. But while our Triton implementation does not fully exploit this, a CUDA backend could.

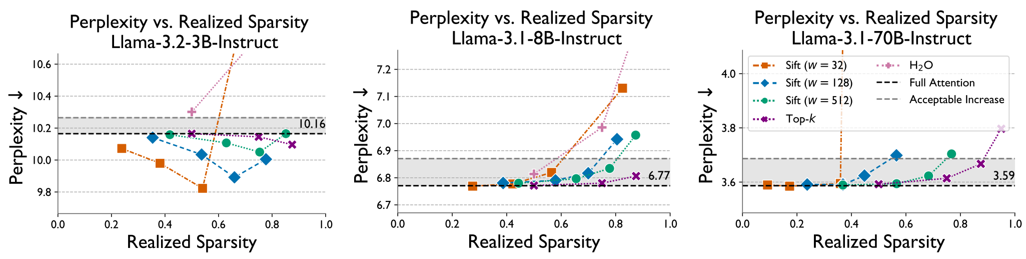

Figure 5: Perplexity evaluation (WikiText-2) comparing SiftAttention with baselines for 3 models

Perplexity Evaluation: We now turn to Figure 5, which compares perplexity on WikiText-2 for SiftAttention, full attention, and other baselines across three Llama models. Focusing on Llama-3.1-8B-Instruct (center), we see that longer warmup phases yield better perplexity for SiftAttention, due to improved power-law fits. A short warmup of 32 steps (orange curve) leads to a noticeable degradation, while warmups of 128 and 512 (green, blue) keep degradation within 0.1 [27] for most sparsity levels, rising to 0.2 only at the highest sparsity. H_2O performs worst, with drops exceeding 0.5. Top-k maintains consistently strong performance, even at the highest realized sparsity values. However, with a sufficient warmup, SiftAttention approaches Top-k performance closely. Similar trends are observed for Llama-3.1-70B-Instruct (right). Interestingly, for Llama-3.2-3B-Instruct (left), both SiftAttention and Top-k achieve lower perplexity than the full attention baseline, with SiftAttention outperforming Top-k. Across all models, SiftAttention remains in the acceptable range of perplexity degradation for most sparsity levels. Results for other models are similar and can be found in appendix B.

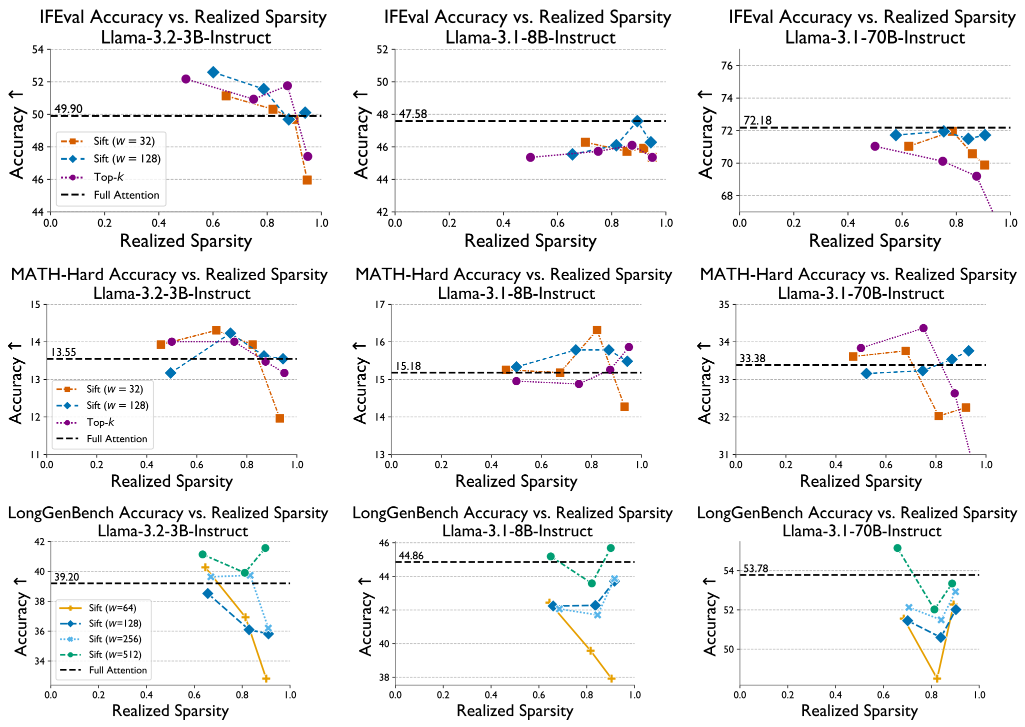

Figure 6: Short (IFEval, MATH) and long (LongGenBench) generation evaluation across 3 models

Downstream Generative Task Evaluation: Finally, we evaluate SiftAttention on downstream generative tasks—IFEval, MATH-Hard, and LongGenBench—shown in Figure 6. IFEval and MATH-Hard involve shorter generation lengths (up to 1280 and 1024 tokens), while LongGenBench requires generating up to 4096 tokens. For IFEval (top row), focusing on Llama-3.2-3B-Instruct (left), we see that SiftAttention outperforms the Top-k baseline given a sufficient warmup of 128 steps (blue curve), especially at high realized sparsities. This trend is consistent across the other models. On MATH-Hard (middle row), a similar trend can be observed, SiftAttention closely matching or outperforming the Top-k baseline. particularly, for Llama-3.1-70B-Instruct, we see a severe degradation in performance with Top-k at high sparsities, but SiftAttention maintains strong performance. Finally, on LongGenBench (bottom row), SiftAttention maintains strong performance even with the longer generation lengths. The average drop in accuracy is 2-3% with a warmup of 256 steps (teal blue curve) across models at high sparsity values. With 512 warmup steps, it nearly matches the full attention baseline.

Together with the perplexity results, these findings highlight SiftAttention's ability to retain strong task performance across models and sparsity levels, often outperforming Top-k, while being easier to parallelize on GPUs.

7 Conclusion

This work introduces SiftAttention, a dynamic power-law guided sparse attention algorithm that reduces GPU memory movement between HBM and SRAM. We observe that attention score quantiles follow a predictable power-law decay over generation steps, consistently across models and datasets - a novel finding that can motivate future work in sparse attention methods. Leveraging this insight, SiftAttention uses a brief warmup phase to fit a power-law model, then predicts thresholds to prune attention scores without requiring costly top-k sorting. Our experiments show that SiftAttention maintains model quality, similar to or better than existing sparse attention techniques, while reducing the data movement between the GPU HBM and SRAM.

7.1 Limitations and Future Work

Our Triton-based implementation of SiftAttention is not fully optimized and performs sub-optimally compared to PyTorch's SDPA kernel. This shortfall arises from inherent limitations in Triton and inefficiencies in sparse vector-matrix multiplication. To address some of these performance issues, we are actively developing a CUDA-based kernel. Additionally, SiftAttention relies on a fixed-length warmup phase, necessitating careful tuning specific to each model and task. An interesting future direction is the exploration of more advanced online fitting techniques, allowing the power-law parameters to be adaptively re-calibrated throughout generation based on discrepancies between predicted and observed attention quantiles. Finally, while our current power-law model is based on post-softmax attention scores, future work could focus on estimating thresholds directly from pre-softmax scores, potentially yielding further computational efficiencies.

References

[1] Introducing triton: Open-source gpu programming for neural networks. `https://openai.com/index/triton/`, 2021.

[2] Dzmitry Bahdanau, Kyunghyun Cho, and Yoshua Bengio. Neural machine translation by jointly learning to align and translate. In Yoshua Bengio and Yann LeCun, editors, *3rd International Conference on Learning Representations, ICLR 2015, San Diego, CA, USA, May 7-9, 2015, Conference Track Proceedings*, 2015.

[3] Konstantin Berestizshevsky, Renzo Andri, and Lukas Cavigelli. Top-theta attention: Sparsifying transformers by compensated thresholding. *arXiv preprint arXiv:2502.08363*, 2025.

[4] Jingxuan Fan, Sarah Martinson, Erik Y Wang, Kaylie Hausknecht, Jonah Brenner, Danxian Liu, Nianli Peng, Corey Wang, and Michael P Brenner. Hardmath: A benchmark dataset for challenging problems in applied mathematics. *arXiv preprint arXiv:2410.09988*, 2024.

[5] Clémentine Fourrier, Nathan Habib, Alina Lozovskaya, Konrad Szafer, and Thomas Wolf. Open llm leaderboard v2. `https://huggingface.co/spaces/open-llm-leaderboard/open_llm_leaderboard`, 2024.

[6] Aaron Grattafiori, Abhimanyu Dubey, Abhinav Jauhri, et al. The llama 3 herd of models, 2024.

[7] Ankit Gupta, Guy Dar, Shaya Goodman, David Ciprut, and Jonathan Berant. Memory-efficient transformers via top-k attention. *CoRR*, abs/2106.06899, 2021.

[8] Andrei Ivanov, Nikoli Dryden, Tal Ben-Nun, Shigang Li, and Torsten Hoefler. Data movement is all you need: A case study on optimizing transformers. *Proceedings of Machine Learning and Systems*, 3:711–732, 2021.

[9] Albert Q Jiang, Alexandre Sablayrolles, Arthur Mensch, Chris Bamford, Devendra Singh Chaplot, Diego de las Casas, Florian Bressand, Gianna Lengyel, Guillaume Lample, Lucile Saulnier, et al. Mistral 7b. *arXiv preprint arXiv:2310.06825*, 2023.

[10] Wonbeom Lee, Jungi Lee, Junghwan Seo, and Jaewoong Sim. InfiniGen: Efficient generative inference of large language models with dynamic KV cache management. In *18th USENIX Symposium on Operating Systems Design and Implementation (OSDI 24)*, pages 155–172, Santa Clara, CA, July 2024. USENIX Association.

[11] Zheng Li, Soroush Ghodrati, Amir Yazdanbakhsh, Hadi Esmaeilzadeh, and Mingu Kang. Accelerating attention through gradient-based learned runtime pruning. In *Proceedings of the 49th Annual International Symposium on Computer Architecture*, pages 902–915, 2022.

[12] Zichang Liu, Aditya Desai, Fangshuo Liao, Weitao Wang, Victor Xie, Zhaozhuo Xu, Anastasios Kyrillidis, and Anshumali Shrivastava. Scissorhands: Exploiting the persistence of importance hypothesis for llm kv cache compression at test time. *arXiv preprint arXiv:2305.17118*, 2023.

[13] Stephen Merity, Caiming Xiong, James Bradbury, and Richard Socher. Pointer sentinel mixture models. *CoRR*, abs/1609.07843, 2016.

[14] Yury Nahshan, Joseph Kampeas, and Emir Haleva. Linear log-normal attention with unbiased concentration. *arXiv preprint arXiv:2311.13541*, 2023.

[15] NVIDIA. Nvidia nsight compute. `https://developer.nvidia.com/nsight-compute`.

[16] Adam Paszke, Sam Gross, Soumith Chintala, Gregory Chanan, Edward Yang, Zachary DeVito, Zeming Lin, Alban Desmaison, Luca Antiga, and Adam Lerer. Automatic differentiation in pytorch. 2017.

[17] Colin Raffel, Noam Shazeer, Adam Roberts, Katherine Lee, Sharan Narang, Michael Matena, Yanqi Zhou, Wei Li, and Peter J. Liu. Exploring the limits of transfer learning with a unified text-to-text transformer, 2023.

[18] Luka Ribar, Ivan Chelombiev, Luke Hudlass-Galley, Charlie Blake, Carlo Luschi, and Douglas Orr. Sparq attention: Bandwidth-efficient llm inference, 2023.

[19] Siddharth Singh and Abhinav Bhatele. AxoNN: An asynchronous, message-driven parallel framework for extreme-scale deep learning. In *Proceedings of the IEEE International Parallel & Distributed Processing Symposium*, IPDPS '22. IEEE Computer Society, May 2022.

[20] Siddharth Singh, Prajwal Singhania, Aditya Ranjan, John Kirchenbauer, Jonas Geiping, Yuxin Wen, Neel Jain, Abhimanyu Hans, Manli Shu, Aditya Tomar, Tom Goldstein, and Abhinav Bhatele. Democratizing AI: Open-source scalable LLM training on GPU-based supercomputers. In *Proceedings of the ACM/IEEE International Conference for High Performance Computing, Networking, Storage and Analysis*, SC '24, November 2024.

[21] Siddharth Singh, Prajwal Singhania, Aditya K. Ranjan, Zack Sating, and Abhinav Bhatele. A 4d hybrid algorithm to scale parallel training to thousands of gpus, 2024.

[22] Prajwal Singhania, Siddharth Singh, Shwai He, Soheil Feizi, and Abhinav Bhatele. Loki: Low-rank keys for efficient sparse attention. In A. Globerson, L. Mackey, D. Belgrave, A. Fan, U. Paquet, J. Tomczak, and C. Zhang, editors, *Advances in Neural Information Processing Systems*, volume 37, pages 16692–16723. Curran Associates, Inc., December 2024.

[23] PyTorch Team. Pytorch 2.0: Our next generation release that is faster, more pythonic and dynamic as ever. `https://pytorch.org/get-started/pytorch-2.0/`, 2023.

[24] Ashish Vaswani, Noam Shazeer, Niki Parmar, Jakob Uszkoreit, Llion Jones, Aidan N Gomez, Łukasz Kaiser, and Illia Polosukhin. Attention is all you need. In *Advances in neural information processing systems*, pages 5998–6008, 2017.

[25] Yuhao Wu, Ming Shan Hee, Zhiqing Hu, and Roy Ka-Wei Lee. Longgenbench: Benchmarking long-form generation in long context llms. *arXiv preprint arXiv:2409.02076*, 2024.

[26] An Yang, Baosong Yang, Beichen Zhang, Binyuan Hui, Bo Zheng, Bowen Yu, Chengyuan Li, Dayiheng Liu, Fei Huang, Haoran Wei, et al. Qwen2. 5 technical report. *arXiv preprint arXiv:2412.15115*, 2024.

[27] Zhewei Yao, Xiaoxia Wu, Cheng Li, Stephen Youn, and Yuxiong He. Zeroquant-v2: Exploring post-training quantization in llms from comprehensive study to low rank compensation. 2023.

[28] Jingrong Zhang, Akira Naruse, Xipeng Li, and Yong Wang. Parallel top-k algorithms on gpu: A comprehensive study and new methods. In *Proceedings of the International Conference for High Performance Computing, Networking, Storage and Analysis*, SC '23, New York, NY, USA, 2023. Association for Computing Machinery.

[29] Zhenyu Zhang, Ying Sheng, Tianyi Zhou, Tianlong Chen, Lianmin Zheng, Ruisi Cai, Zhao Song, Yuandong Tian, Christopher Ré, Clark Barrett, et al. H _2 o: Heavy-hitter oracle for efficient generative inference of large language models. *arXiv preprint arXiv:2306.14048*, 2023.

[30] Jeffrey Zhou, Tianjian Lu, Swaroop Mishra, Siddhartha Brahma, Sujoy Basu, Yi Luan, Denny Zhou, and Le Hou. Instruction-following evaluation for large language models, 2023.

A Extended Power-Law Analysis Results

A.1 Power-Law Samples

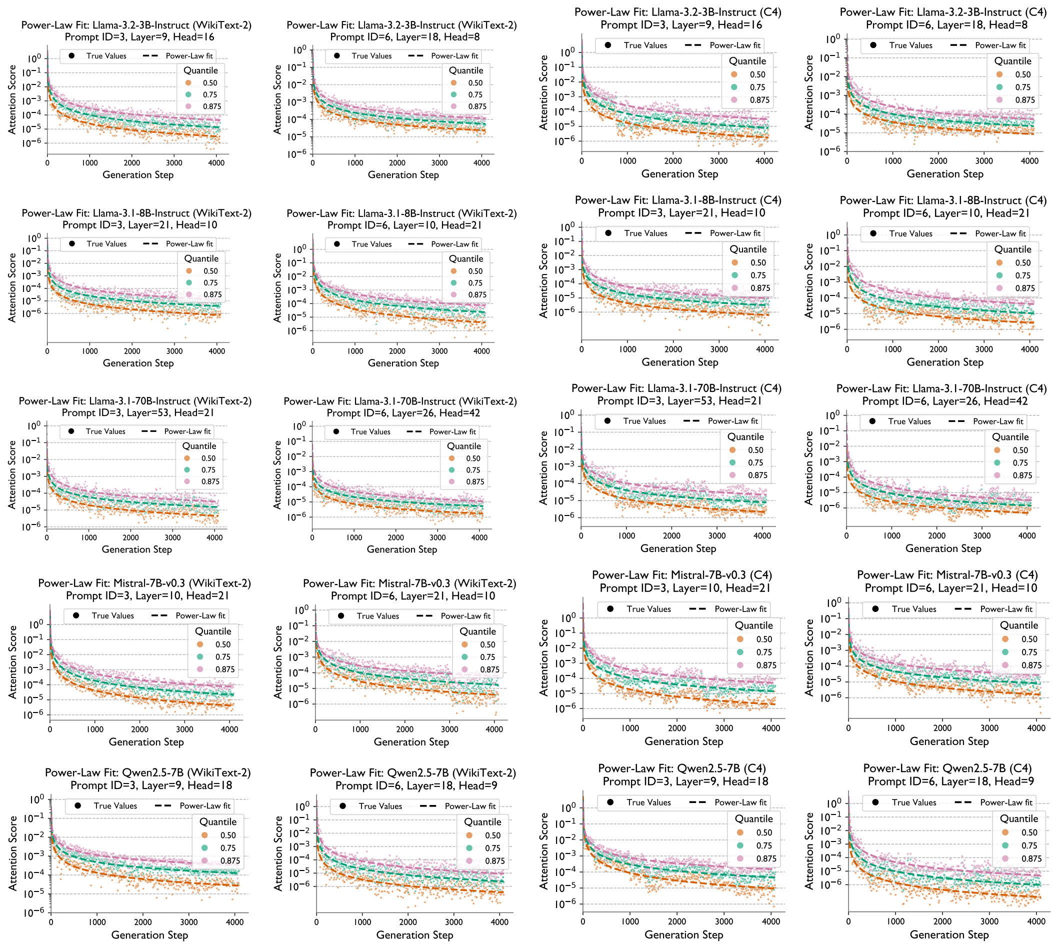

Figure 7: Power-Law fit for attention score quantiles (log y-scale) over generation steps across 5 different models. The two left columns are samples on WikiText-2, and the two right columns are samples on C4.

In this section, we present extended results from our power-law analysis of attention score quantiles. Figure 7 displays representative samples of the observed quantiles across various models, datasets, prompts, layers, and attention heads. These qualitative results suggest that a power-law trend can often be visually inferred from the evolution of attention score quantiles. While the trend appears weaker in some samples from the C4 dataset, this may be attributable to suboptimal sample selection rather than a lack of underlying structure.

Although this analysis is not exhaustive, it offers evidence that power-law behavior is a consistent characteristic of attention score distributions. As reported in Figure 2 of the main text, the R^2 values—indicating the goodness-of-fit for the power-law model—consistently exceed 0.6 across all evaluated models and datasets. Notably, the C4 dataset exhibits tighter variance in R^2 values.

A.2 Power-Law Fitting with Warmup

In this section, we further investigate how the length of the warmup period affects the estimation of the power-law fit parameters, for a perplexity evaluation task.

Figure 8 shows a clear correlation between warmup length and power-law fit quality. With shorter warmup periods (e.g., 64 steps), we observe significantly lower R^2 scores—often dropping into

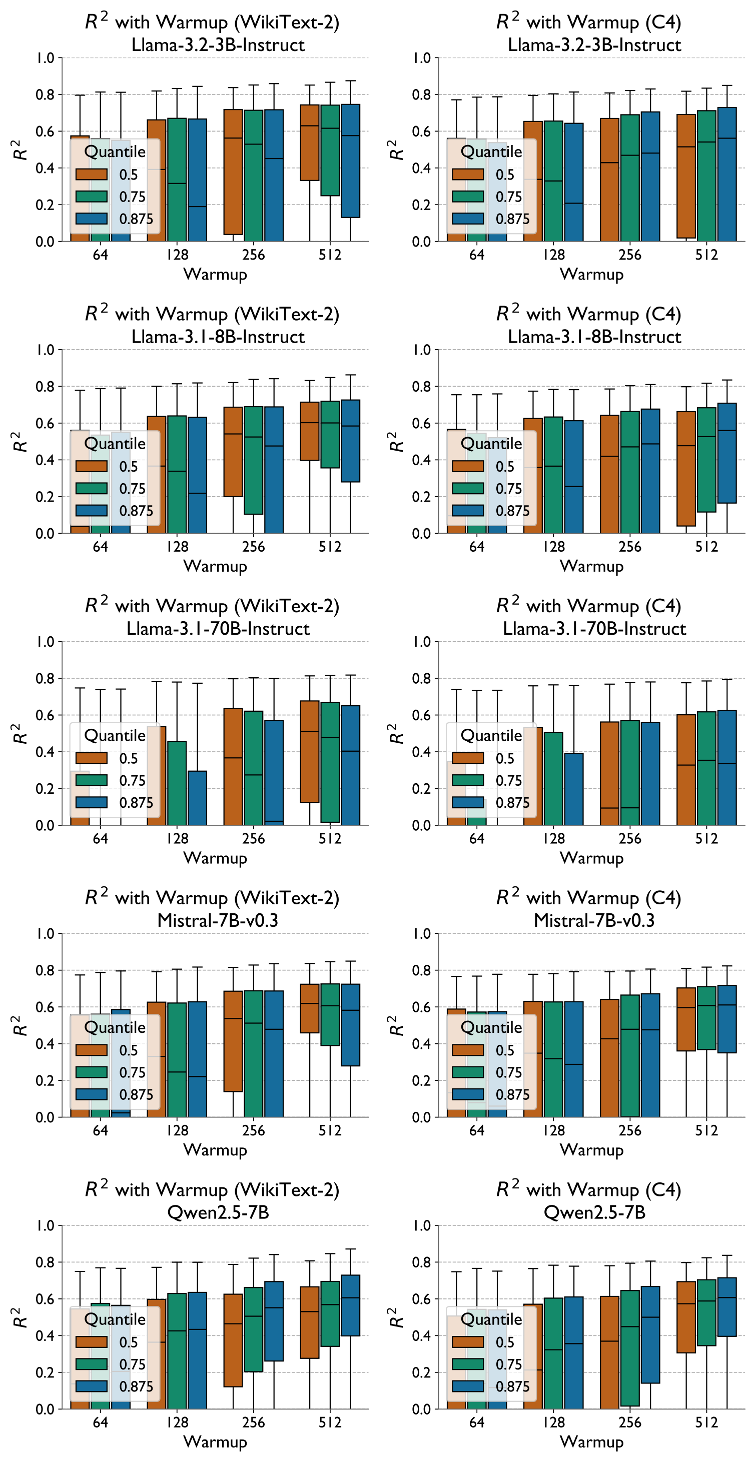

Figure 8: R^2 distribution across 5 different models, evaluated across warmup sizes w: 64, 128, 256, and 512 steps. Left columns are samples on WikiText-2; right columns are samples on C4

negative values. These negative values indicate that the power-law fit performs worse than a naive model that simply predicts the mean of the log-quantile values, especially highlighting unreliable parameter estimation with short warmup periods. This degradation is especially evident in the C4 dataset, where initial R^2 scores are consistently lower than those observed on WikiText-2.

As the warmup length increases, the fit quality steadily improves across all datasets. By 512 warmup steps, R^2 values become consistently positive and substantially higher, indicating that a longer warmup allows for more accurate modeling of the attention score quantile decay. This trend underscores the importance of allocating a sufficient warmup period for reliable threshold estimation in SiftAttention. We also observe that the fit quality is better on WikiText-2 than on C4. While these results demonstrate the feasibility of the warmup approach in SiftAttention, we acknowledge that the fitting accuracy could be improved. More sophisticated power-law fitting algorithms could be explored in future work, to bridge the gap in estimating the real power-law trend with a high R^2 (as shown in the previous section). One possible approach could explore using realized sparsity signals to implement an adaptive warmup schedule

Despite occasional poor fit quality, we observe strong downstream performance even with shorter warmup lengths, as shown in Section 6 and Appendix B. We hypothesize that this robustness arises because, although the realized sparsity may deviate from the intended target, the model still retains a meaningful and consistent subset of top-τ attention scores. In effect, the power-law may be accurately modeling a different effective sparsity level than initially specified.

Another limitation of this analysis is that we only analyze the power-law fit on a perplexity task. We observe that the gap between realized and intended sparsity is larger on perplexity evaluation than on other tasks such as IFEval and MATH. We hypothesize that these results are linked and that the same analysis performed on other tasks like IFEval and MATH could yield significantly better R^2 scores.

B Detailed Evaluation Results

B.1 Realized vs. Intended Sparsity

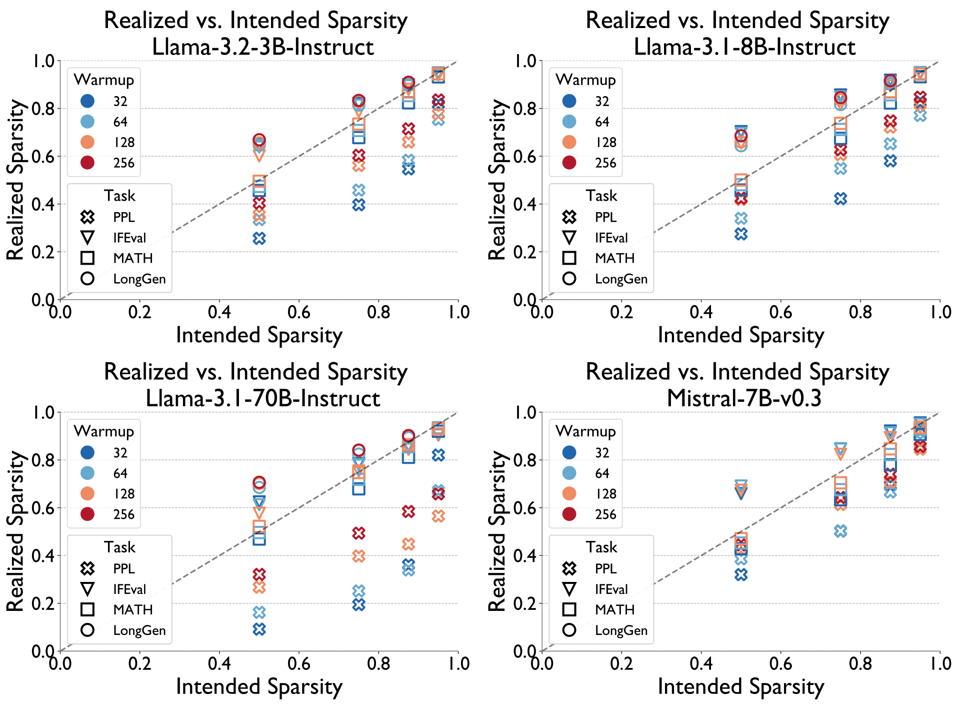

Figure 9: Intended vs. Realized sparsity on SiftAttention across tasks and warmup lengths for 5 different models.

In this section we analyze the relationship between intended and realized sparsity for SiftAttention across multiple models, tasks, and warmup lengths, as shown in Figure 9. We observe that the disparity between intended and realized sparsity varies significantly across models. Generation tasks consistently demonstrate realized sparsity closer to the intended sparsity, suggesting a potential relationship between task type and sparsity behavior. This trend warrants further investigation.

Notably, the Llama-3.1-70B model exhibits a weaker correlation between realized and intended sparsity compared to smaller models. While this could indicate different underlying dynamics in larger models, these results are not conclusive and require additional study to fully understand the scaling behavior of attention patterns.

The effectiveness of SiftAttention is evident across all models: increasing the warmup length consistently brings realized sparsity closer to intended levels. Furthermore, we observe that increasing the intended sparsity hyper-parameter (specified by the τ-th quantile) leads to proportional increases in realized sparsity, demonstrating the method's ability to effectively control sparsification across different scales and architectures.

B.2 Perplexity Evaluation

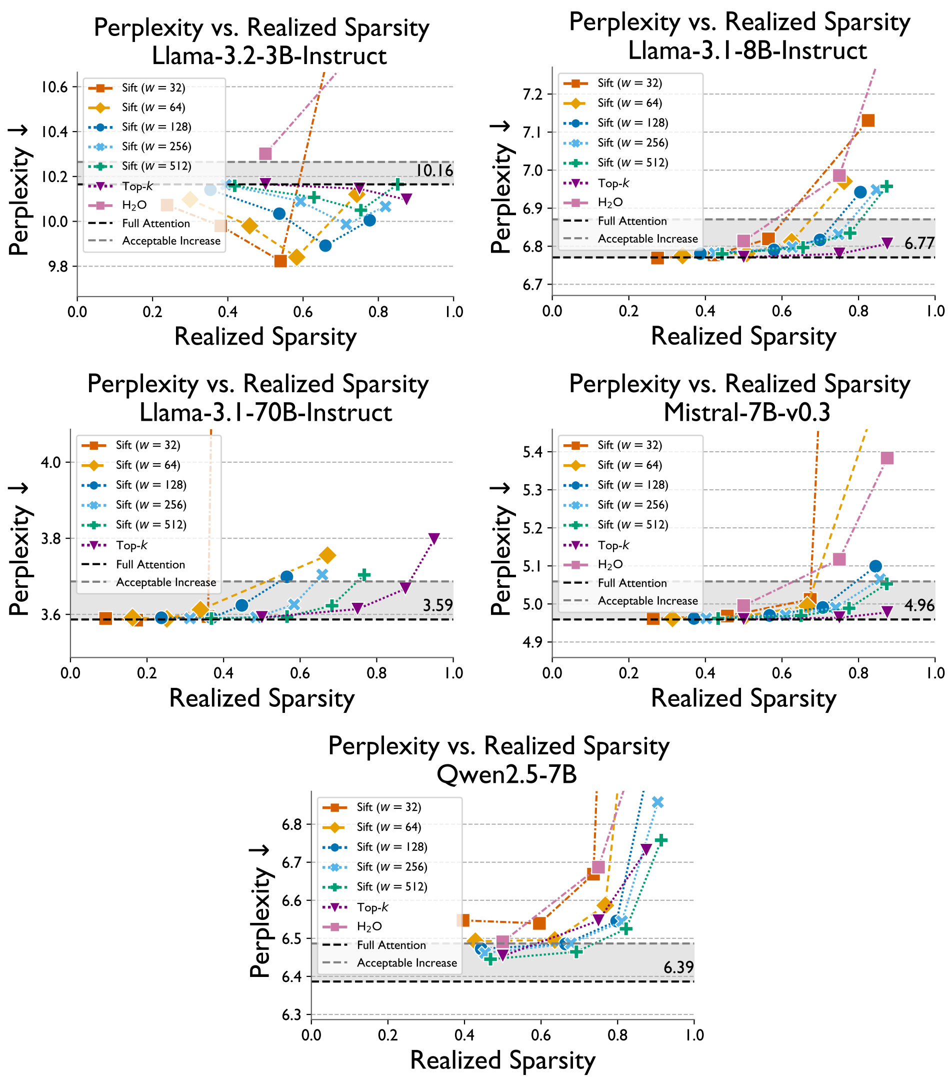

Figure 10: Perplexity evaluation (WikiText-2) comparing SiftAttention with baselines across 5 models

Figure 10 presents the perplexity evaluation results on WikiText-2 across five different models. Consistent with the results shown in Figure 5 of the main text, we find that SiftAttention achieves perplexity comparable to or better than the Top-k baseline (dark purple). The H_2O method (light pink) performs the worst, with the perplexity degradation exceeding acceptable levels—even at low realized sparsity. Additionally, we observe that across all models, longer warmup lengths correlate with improved perplexity, underscoring the importance of sufficient warmup for accurate threshold estimation.

B.3 Short Context Tasks

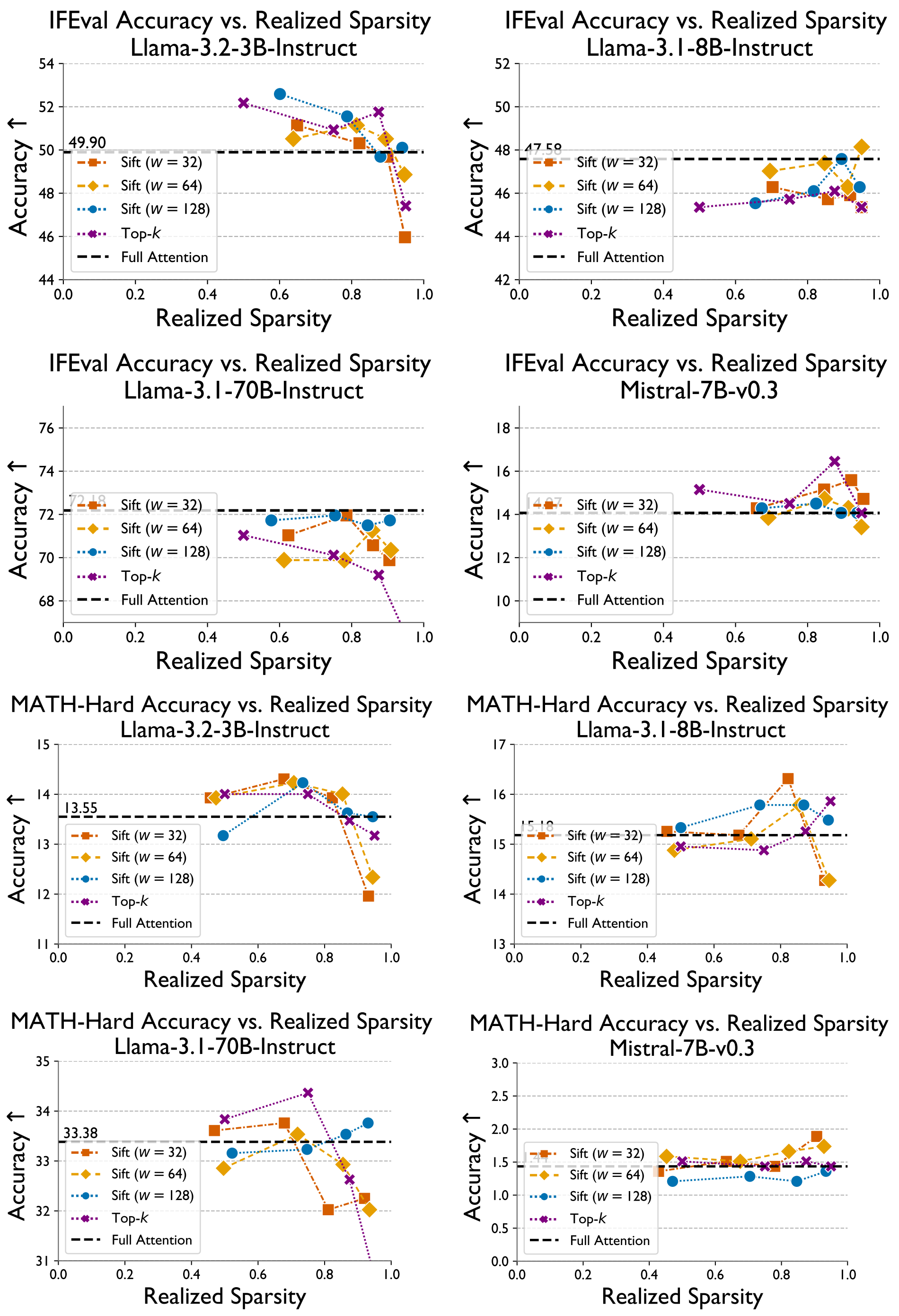

Figure 11: SiftAttention short-context task performance vs. Realized Sparsity on IFEval and MATH-Hard across 4 different models

In this section, we present detailed results for our short-context task evaluation. Figure 11 illustrates the performance of SiftAttention on the IFEval (top two rows) and MATH-Hard (bottom two rows) tasks across four different models. For the IFEval task, we observe that with a warmup length of $w = 128$, SiftAttention consistently outperforms the Top-k baseline (dark purple) across all Llama models, and matches its performance on the Mistral model at high realized sparsity levels. A similar trend holds for the MATH-Hard task, with one exception: on Llama-3.1-8B, SiftAttention performs slightly worse than Top-k at the highest sparsity levels, but still surpasses the Full Attention baseline. Notably, for Llama-3.1-70B, Top-k accuracy degrades significantly at high sparsity, whereas SiftAttention maintains performance close to the Full Attention baseline.

B.4 Runtime and Data Transfer Evaluation

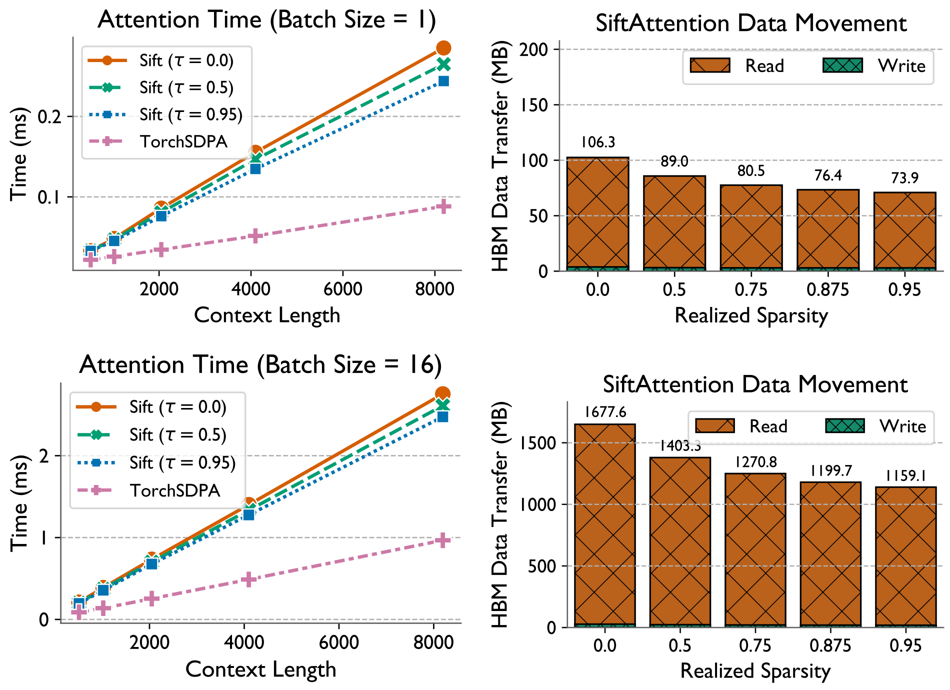

Figure 12: Post-warmup attention latency of our Triton-based SiftAttention implementation compared to PyTorch's fused SDPA across varying context lengths for batch size 1 (top-left) and 16 (bottom-left). HBM data transfer volume as a function of realized sparsity (Context Length = 8192) for batch size 1 (top-right) and 16 (bottom-right).

Figure 12 presents the post-warmup attention latency of our implementation compared to PyTorch's fused SDPA kernel, evaluated across varying context lengths for two batch sizes: 1 (top-left) and 16 (bottom-left). The trends observed here are consistent with those in Figure 4 from the main text, which reports results for batch size 8. As expected, increasing the sparsity level reduces attention latency with SiftAttention. However, our current kernel implementation is approximately 2-3$\times$ slower than PyTorch's highly optimized fused SDPA. The corresponding HBM data transfer volume is shown in the top-right and bottom-right subplots. Again, we observe that higher sparsity leads to reduced HBM traffic, confirming that SiftAttention effectively reduces memory bandwidth usage, which is the reason for the decrease in attention latency with higher sparsity.

B.5 Visualization of Sparsity Masks

In this section, we visualize the attention sparsity patterns for two intended sparsity levels: $\tau = 0.5$ and $\tau = 0.9$, during the generation of a 4096-token sequence using Llama-3.1-8B-Instruct. Figure 13 displays the sparsity masks at the 2048th generation step. As expected, increasing the intended sparsity level results in a sparser attention pattern—evidenced by the greater prevalence of blacked-out (masked) tokens in the lower panel. All tokens beyond the 2048th position are masked (shown in black) as they represent future positions and are therefore not attended to.

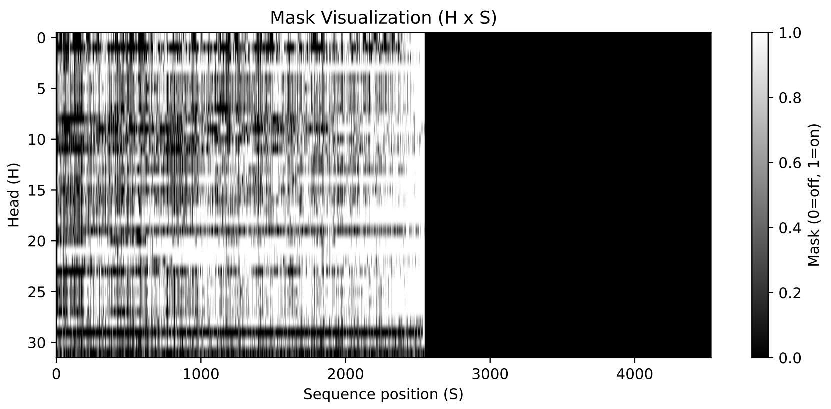

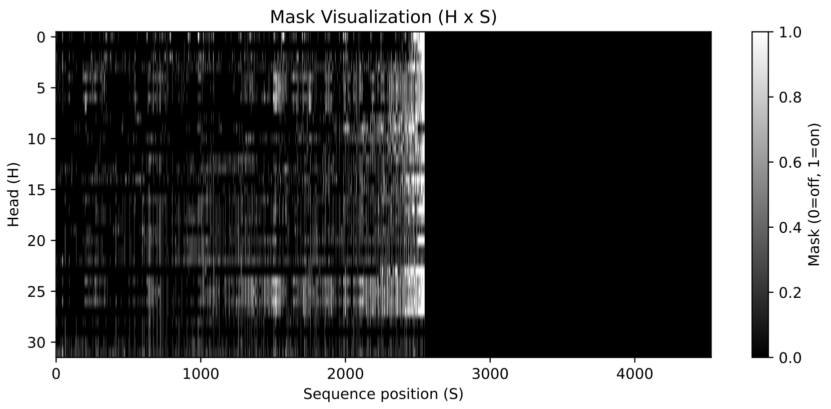

Figure 13: Sparsity masks for $\tau = 0.5$ (top) and $\tau = 0.9$ (bottom) at the 2048^{th} generation step when generating a sequence of 4096 tokens using Llama-3.1-8B-Instruct. The blacks represent the tokens not attended to, while the white represents the tokens that are attended to.

C Generation Sample

In this section, we present sample outputs generated using SiftAttention with the Llama-3.1-8B-Instruct model under two different hyperparameter configurations.

Prompt

In a world where technology has advanced beyond imagination, society grapples with the consequences of its own creations. The integration of artificial intelligence into everyday life has revolutionized how we live, work, and interact. However, with great power comes great responsibility, and ethical dilemmas abound. Governments struggle to regulate the use of AI, while corporations push the boundaries of what is possible in the pursuit of profit. Meanwhile, individuals navigate a landscape where privacy is increasingly scarce, and the line between human and machine blurs. Against this backdrop, a new generation of thinkers emerges, questioning the very nature of consciousness and what it means to be human. As tensions rise and alliances shift, the fate of humanity hangs in the balance, waiting to be written by those bold enough to seize the pen of destiny.

Llama-3.1-8B-Instruct — Full Attention:

In this world, the future is not set in stone, but forged in the fire of human ingenuity and the choices we make today. The question is, what will we create? And what will we become? Join us on a journey through the uncharted territories of the future, where the boundaries of reality are pushed to their limits, and the possibilities are endless. Welcome to the world of tomorrow, where the only constant is change, and the only truth is that the future is what we make it. Explore the latest developments in AI, robotics, and biotechnology, and discover the innovations that are shaping the world of tomorrow. From the rise of the gig economy to the emergence of new forms of governance, we'll delve into the complex issues that are redefining the human experience. Join the conversation and become a part of the future that's being written. The world of tomorrow is not just a prediction - it's a choice. What will you create? What will you become? The future is in your hands.

Llama-3.1-8B-Instruct — SiftAttention $w = 16$, $\tau = 0.875$

In this world, the future is not set in stone, but forged in the fire of human ingenuity and the choices we make. The question is, what will we create next? Will we build a utopia or a dystopia? The choice is ours. The future is now. The world is a complex tapestry of human and artificial intelligence, and the story of what comes next is being written by us, in this moment. Join us on this journey into the unknown, where the boundaries of what is possible are pushed to the limit. The future is a blank page, waiting to be filled with the stories of those who dare to imagine. In this world, the future is not just a destination, but a creation. And the creation of the future is in our hands.

Llama-3.1-8B-Instruct — SiftAttention $w = 32$, $\tau = 0.95$

In this world, the future is not set in stone, but forged in the fire of human ingenuity and the choices we make today. The question is, what will we create tomorrow? The future is in our hands. The future is in our code. The future is in our choices. The future is now. The future is... (To be continued)